

Electronic supplementary information

for

Targeted synthesis of a Cr^{III}–O–V^V core oxo-bridged complex: spectroscopic, magnetic and electrical properties

Lidija Androš Dubraja,^{*a} Dijana Žilić,^a Kristina Olujić,^a Luka Pavić,^a Krešimir Molčanov^a
and Damir Pajić^b

^aRuđer Bošković Institute, Bijenička cesta 54, 10000 Zagreb, Croatia

^bDepartment of Physics, Faculty of Science, University of Zagreb, Bijenička cesta 32, 10000
Zagreb, Croatia

Email: Lidija.Andros@irb.hr

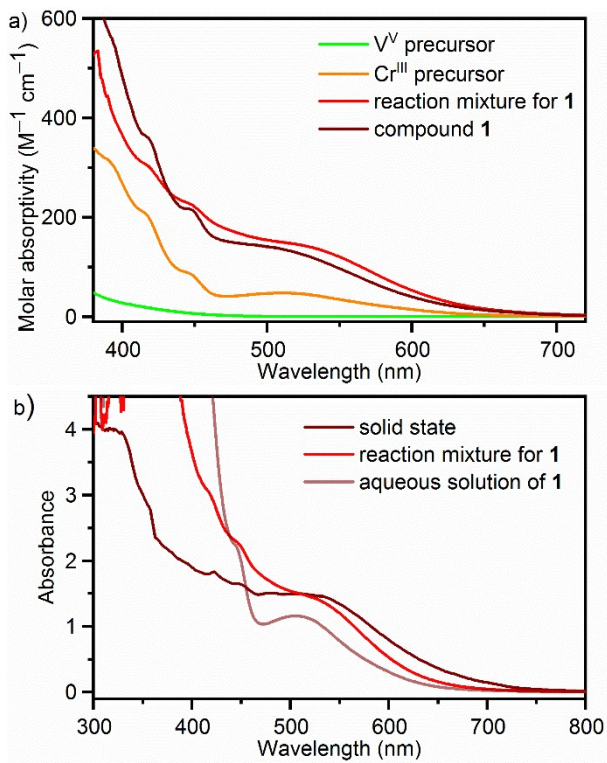


Figure S1. a) Electronic absorption spectra ($c = 10 \text{ mM}$) of aqueous solutions containing: $[\text{VO}_2(\text{C}_2\text{O}_4)_2]^{3-}$ precursor, $[\text{Cr}(\text{bpy})_2(\text{H}_2\text{O})_2]^{3+}$ precursor, reaction mixture for the synthesis of **1** and complex **1**; b) Comparison between solid-state UV-visible diffuse reflectance spectrum of the compound $[\text{Cr}(\text{bpy})_2(\text{H}_2\text{O})(\mu-\text{O})\text{VO}(\text{C}_2\text{O}_4)_2]_2 \cdot 9\text{H}_2\text{O}$ (**1**) and absorbance spectrum of reaction mixture for **1** and aqueous solution of **1**. The values of diffuse reflectance spectrum are converted to pseudoabsorbance spectra using the Kubelka-Munk transformation.

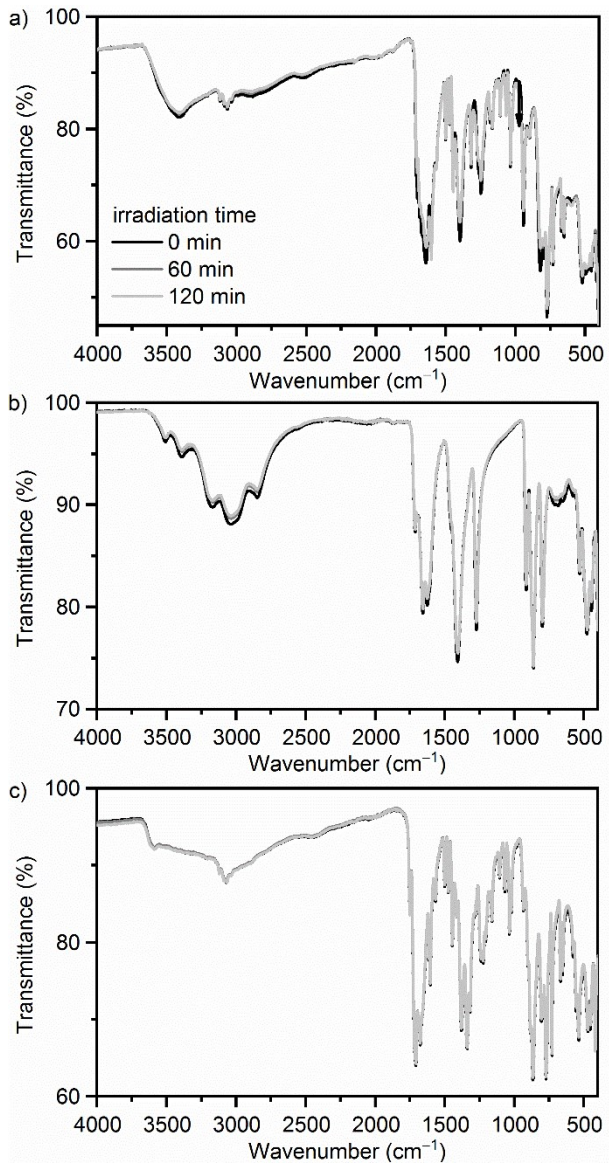


Figure S2. Irradiation-time dependence of ATR spectrum for: a) compound $[\text{Cr}(\text{bpy})_2(\text{H}_2\text{O})(\mu\text{-O})\text{VO}(\text{C}_2\text{O}_4)_2]_2 \cdot 9\text{H}_2\text{O}$ (1); b) compound $(\text{NH}_4)_3[\text{VO}_2(\text{C}_2\text{O}_4)_2] \cdot \text{H}_2\text{O}$; c) compound $[\text{Cr}(\text{bpy})_2(\text{H}_2\text{O})(\mu\text{-O})\text{TaO}(\text{C}_2\text{O}_4)_3]_2 \cdot 3.5\text{H}_2\text{O}$. Spectra are recorded at 298 K *in situ* at 0 (black line), 60 (grey line) and 120 min (lighter grey line) of irradiation with white (LED) light.

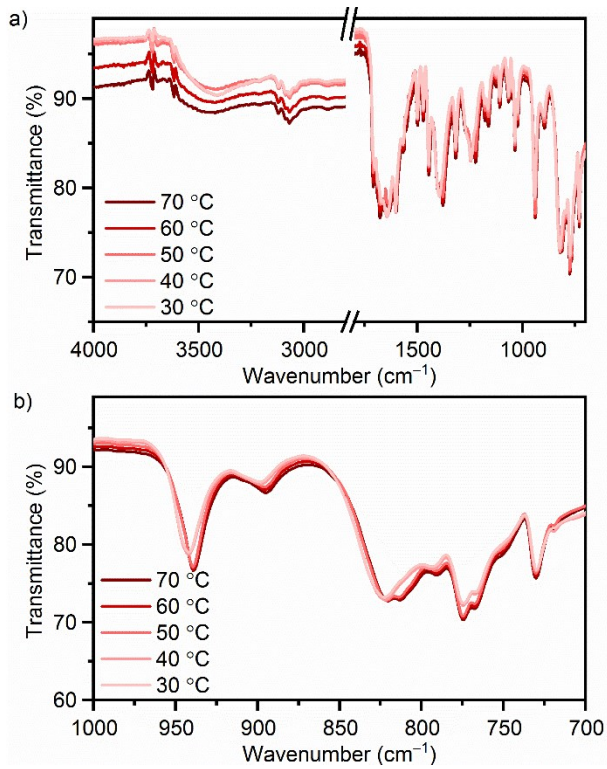


Figure S3. Temperature dependence of ATR spectrum for compound $[\text{Cr}(\text{bpy})_2(\text{H}_2\text{O})(\mu-\text{O})\text{VO}(\text{C}_2\text{O}_4)_2] \cdot 9\text{H}_2\text{O}$ (1): a) mid-IR range; b) range where significant bands related to metal-oxo bond vibrations appear.

Table S1. Crystallographic data and structure refinement details for $[\text{Cr}(\text{bpy})_2(\text{H}_2\text{O})(\mu\text{-O})\text{VO}(\text{C}_2\text{O}_4)_2]_2 \cdot 9\text{H}_2\text{O}$ (**1**)

T/K	109(2)
Crystal colour, habit	Dark red, prism
Empirical formula	$\text{C}_{48}\text{H}_{54}\text{Cr}_2\text{V}_2\text{N}_8\text{O}_{31}$
Formula weight/g mol ⁻¹	1444.87
Crystal system	Triclinic
Space group	$P\bar{1}$
<i>a</i> /Å	12.4561(6)
<i>b</i> /Å	17.1390(5)
<i>c</i> /Å	13.9847(7)
α /°	92.281(3)
β /°	81.867(4)
γ /°	96.178(3)
<i>V</i> /Å ³	2937.4(2)
<i>Z</i>	2
ρ_{calcd} /g cm ⁻³	1.634
μ /mm ⁻¹	6.452
<i>F</i> (000)	1480
θ range/°	3.19–76.50
Measured reflections	20985
Independent reflections	10868
Observed reflections	7303
No. of parameters, restraints	886,34
<i>R</i> _{int}	0.0745
<i>R</i> , w <i>R</i> [<i>I</i> > 2σ(<i>I</i>)]	0.0690, 0.1850
<i>R</i> , w <i>R</i> [all data]	0.1004, 0.2125
Goodness of fit, <i>S</i>	1.028
$\Delta\rho_{\text{max}}, \Delta\rho_{\text{min}}$ /e Å ⁻³	0.686; -0.947

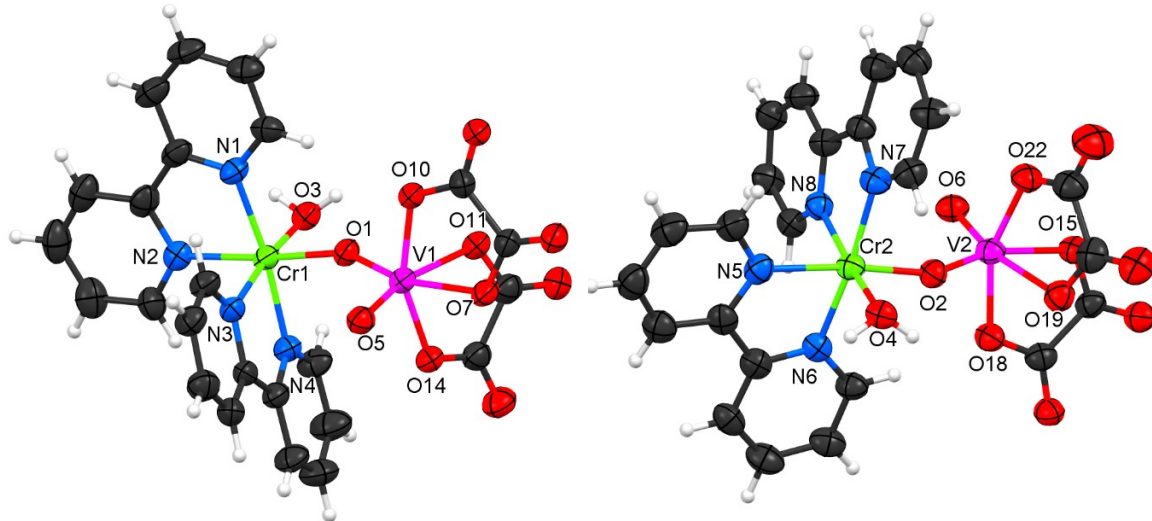


Figure S4. Two crystallographically independent dinuclear Cr1–O1–V1 and Cr2–O2–V2 units in compound 1. Displacement ellipsoids are drawn for the probability of 50 % and hydrogen atoms are shown as spheres of arbitrary radii.

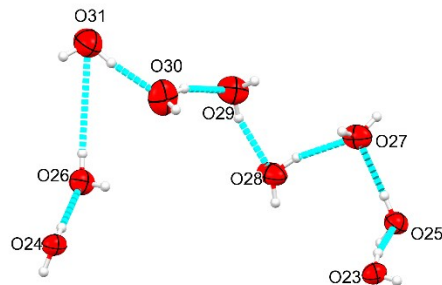


Figure S5. Nine crystallographically independent water molecules of crystallization connected through hydrogen bonds in compound 1. Displacement ellipsoids are drawn for the probability of 50 % and hydrogen atoms are shown as spheres of arbitrary radii.

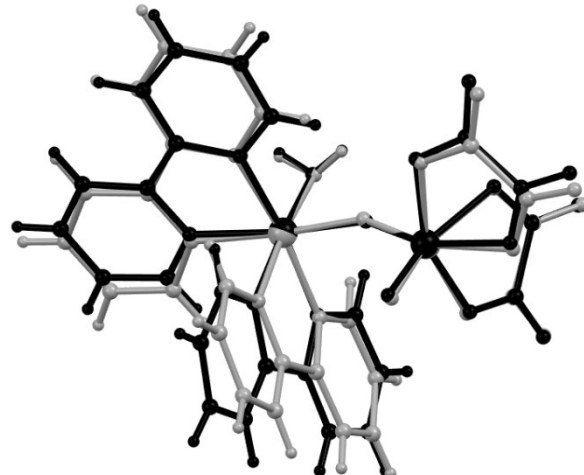


Figure S6. The structural overlay between two crystallographically independent dinuclear Cr1–O1–V1 (black) and Cr2–O2–V2 units (grey).

Table S2. Bond lengths (\AA) involved in the first coordination sphere of V and Cr atoms in **1** at 109(2) K.

V1–O1	1.726(4)	V2–O2	1.707(4)
V1–O5	1.606(4)	V2–O6	1.604(4)
V1–O7	2.088(4)	V2–O15	2.111(4)
V1–O10	1.973(4)	V2–O18	1.985(4)
V1–O11	2.171(4)	V2–O19	2.193(4)
V1–O14	1.992(4)	V2–O22	1.953(4)
Cr1–O1	1.879(4)	Cr2–O2	1.896(4)
Cr1–O3	1.985(4)	Cr2–O4	1.974(4)
Cr1–N1	2.042(5)	Cr2–N5	2.057(5)
Cr1–N2	2.066(5)	Cr2–N6	2.043(5)
Cr1–N3	2.041(4)	Cr2–N7	2.042(5)
Cr1–N4	2.047(4)	Cr2–N8	2.045(6)

Table S3. Selected angles ($^{\circ}$) in the coordination spheres of Cr1 and Cr2 in **1** at 109(2) K.

O1–Cr1–O3	87.90(17)	O2–Cr2–O4	89.53(17)
O1–Cr1–N1	95.81(18)	O2–Cr2–N5	173.22(19)
O1–Cr1–N2	175.38(17)	O2–Cr2–N6	93.87(18)
O1–Cr1–N3	89.68(18)	O2–Cr2–N7	89.79(18)
O1–Cr1–N4	89.86(18)	O2–Cr2–N8	92.74(18)
O3–Cr1–N1	89.88(18)	O4–Cr2–N5	90.32(19)
O3–Cr1–N2	91.22(18)	O4–Cr2–N6	92.53(17)
O3–Cr1–N3	173.20(17)	O4–Cr2–N7	93.06(18)
O3–Cr1–N4	94.70(18)	O4–Cr2–N8	171.98(17)
N1–Cr1–N2	79.64(19)	N5–Cr2–N6	79.4(2)
N1–Cr1–N3	96.69(19)	N5–Cr2–N7	96.99(19)
N1–Cr1–N4	172.8(2)	N5–Cr2–N8	88.33(19)
N2–Cr1–N3	91.69(18)	N6–Cr2–N7	173.3(2)
N2–Cr1–N4	94.74(19)	N6–Cr2–N8	94.99(18)
N3–Cr1–N4	78.94(19)	N7–Cr2–N8	79.3(2)

Table S4. Selected angles ($^{\circ}$) in the coordination spheres of V1 and V2 in **1** at 109(2) K.

O5–V1–O1	104.10(19)	O6–V2–O2	103.7(2)
O5–V1–O10	103.35(19)	O6–V2–O22	94.33(19)
O1–V1–O10–	92.42(17)	O2–V2–O22	99.69(18)
O5–V1–O14	92.71(18)	O6–V2–O18	103.07(19)
O1–V1–O14	99.19(17)	O2–V2–O18	91.32(17)
O10–V1–O14	157.30(17)	O22–V2–O18	156.63(19)
O5–V1–O7	91.27(18)	O6–V2–O15	92.40(19)
O1–V1–O7	163.56(18)	O2–V2–O15	162.21(18)
O10–V1–O7	78.17(15)	O22–V2–O15	86.38(16)
O14–V1–O7	85.63(16)	O18–V2–O15	77.51(15)
O5–V1–O11	165.50(18)	O6–V2–O19	167.83(18)
O1–V1–O11	87.93(18)	O2–V2–O19	86.57(18)
O10–V1–O11	83.88(16)	O22–V2–O19	77.27(17)
O14–V1–O11	77.16(16)	O18–V2–O19	82.93(17)
O7–V1–O11	77.77(17)	O15–V2–O19	78.43(16)

Table S5. Hydrogen–bonding geometry in compound **1** at 109(2) K.

$D\text{--H}\cdots A$	$D\text{--H}/\text{\AA}$	$H\cdots A/\text{\AA}$	$D\cdots A/\text{\AA}$	$D\text{--H}\cdots A/{}^{\circ}$	Symm. op. on A
O3–H3A…O23	0.86(5)	1.80(6)	2.628(6)	160(8)	$1 + x, y, z$
O3–H3B…O17	0.86(4)	1.86(4)	2.686(5)	161(8)	$x, 1 + y, z$
O4–H4A…O9	0.85(4)	1.95(4)	2.719(5)	150(7)	
O4–H4B…O24	0.86(6)	1.77(6)	2.607(6)	165(8)	
O23–H23A…O11	0.85(6)	1.99(6)	2.833(6)	168(8)	$-1 + x, y, z$
O23–H23B…O25	0.85(3)	2.00(4)	2.820(6)	161(8)	$-1 + x, 1 + y, z$
O24–H24A…O19	0.85(6)	2.13(6)	2.966(6)	168(7)	
O24–H24B…O26	0.85(4)	1.95(4)	2.792(6)	171(6)	
O25–H25A…O27	0.86(6)	2.00(6)	2.817(7)	158(6)	$x, -1 + y, z$
O25–H25B…O16	0.86(4)	1.93(4)	2.724(6)	153(6)	
O26–H26A…O8	0.89(5)	1.90(5)	2.791(6)	173(6)	
O26–H26B…O31	0.86(5)	3.23(6)	4.054(8)	161(5)	
O27–H27A…O13	0.86(6)	2.04(6)	2.881(7)	164(6)	$-1 + x, y, z$
O27–H27B…O12	0.86(5)	2.09(7)	2.816(7)	142(6)	$2 - x, -y, 2 - z$
O28–H28A…O15	0.86(6)	1.99(6)	2.852(7)	176(8)	
O28–H28B…O27	0.86(4)	2.04(4)	2.854(7)	158(7)	$x, -1 + y, z$
O29–H29A…O28	0.89(6)	1.95(6)	2.799(9)	160(6)	
O29–H29B…O13	0.88(4)	2.12(4)	2.983(7)	171(6)	$2 - x, -1 - y, 2 - z$
O30–H30A…O29	0.89(7)	2.00(7)	2.850(9)	161(7)	$2 - x, -1 - y, 2 - z$
O30–H30B…O7	0.87(6)	1.89(6)	2.749(7)	168(6)	
O31–H31A…O21	0.88(6)	2.16(7)	2.899(9)	141(6)	$2 - x, -1 - y, 1 - z$
O31–H31B…O30	0.89(6)	1.89(6)	2.736(10)	158(6)	

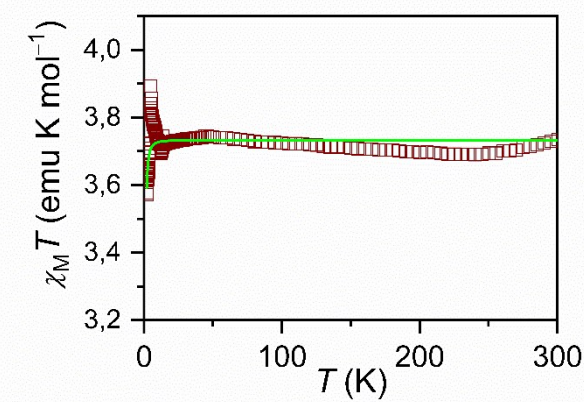


Figure S7. The temperature dependence of the product of susceptibility and temperature for compound **1** (calculated per two Cr atoms) measured in the field of 1000 Oe. The solid green line represents the corresponding fitting curve according to Van Vleck formula.

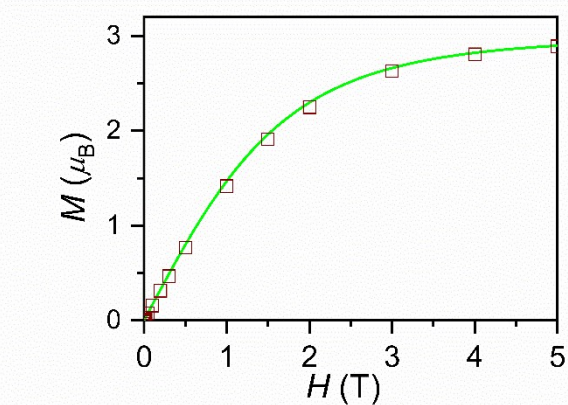


Figure S8. Molar magnetization (M) as a function of applied magnetic field (H) at 2 K (open symbols). The green line represents the Brillouin function at 2 K employing $g_{\text{Cr}} = 1.98$.

Table S6. The fitting parameters obtained from equivalent circuit modelling of complex impedance spectra measured at room temperature for compound **1**.

R_g / Ω	CPEg		C_g^a / F
	$A_g / s^a \Omega^{-1}$	a_g	
1.32×10^8	9.69×10^{-12}	0.96	7.34×10^{-12}
R_{gb} / Ω	CPEgb		C_{gb}^a / F
	$A_{gb} / s^a \Omega^{-1}$	a_{gb}	
1.17×10^9	9.31×10^{-11}	0.67	3.12×10^{-11}
CPE			
$A / s^a \Omega^{-1}$		a	
7.80×10^{-9}		0.37	

* Capacity (C) calculated from the equation: $C = A(\omega_{max})^{\alpha-1}$

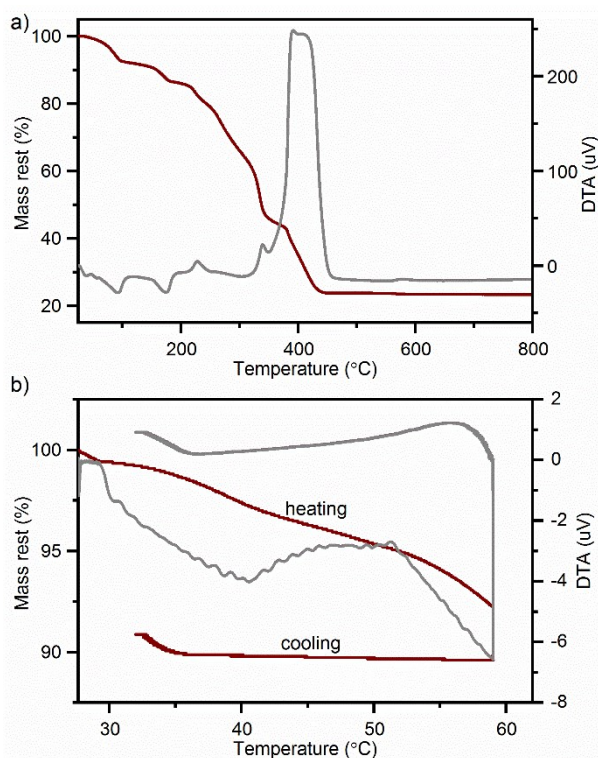


Figure S9. Thermal behaviour of compound $[\text{Cr}(\text{bpy})_2(\text{H}_2\text{O})(\mu\text{-O})\text{VO}(\text{C}_2\text{O}_4)_2]_2 \cdot 9\text{H}_2\text{O}$ (**1**) in a synthetic air atmosphere: a) TG/DTA curve measured in the range from RT to 1000 °C with heating rate 10 °C/min; b) TG/DTA curve measured in the range from RT to 60 °C with heating rate 2 °C/min.

Table S7. Termogrammetric data for decompositon of compound $[\text{Cr}(\text{bpy})_2(\text{H}_2\text{O})(\mu\text{-O})\text{VO}(\text{C}_2\text{O}_4)_2]_2 \cdot 9\text{H}_2\text{O}$ (**1**) in a synthetic air atmosphere (shown in Figure 9).

$\Delta T / ^\circ\text{C}$	w / %		Loss	DTA _{peak} / °C
	exp.	calcd.		
heating rate 2 °C/min				
30–60	10.39	11.21	9H ₂ O (crystallization water molecules)	42, 62 endo
heating rate 10 °C/min				
40–185	13.54	13.71	11H ₂ O	92, 175 endo
195–380	43.70	43.24	4bpy	228, 340 exo
380–600	19.69	19.95	4CO + 4CO ₂	392, 415 exo
Residue CrVO ₄				
	exp.	calcd.		
	23.07	23.10		